Conformational landscapes of rigid and flexible molecules explored with variable temperature ion mobility-mass spectrometry

Xudong Wang[1], Emma Norgate[1], Junxiao Dai[1], Florian Benoit[1], Jason Kalapothakis[1], Tony Bristow[2], Richard M. England[3] and Perdita E. Barran[1,*]

[1]Michael Barber Centre for Collaborative Mass Spectrometry, Manchester Institute of Biotechnology, Department of Chemistry, The University of Manchester, 131 Princess Street, Manchester, M1 7DN, UK. [2]Chemical Development, Pharmaceutical Technology and Development, Operations, AstraZeneca, Charter Way, Macclesfield, SK102NA, UK. [3]Advanced Drug Delivery, Pharmaceutical Sciences, R&D, AstraZeneca, Macclesfield, SK10 2NA.

[*]Corresponding Author: perdita.barran@manchester.ac.uk

Abstract

Understanding the effect of temperature to the structural integrity and dynamics of proteins has relevance for many areas including biotechnology and the maintenance of a stable food supply for the climate emergency. The methods that can explore changes in structure as a function of sub-ambient temperature are scant, and yet many drugs are stored at such temperatures. Here we show how variable temperature ion mobility-mass spectrometry (VT-IM-MS) can provide the role of temperature on conformational landscapes in the form of collision cross sections at discrete temperatures. To delineate collision effects from structural change we report measurements made on four molecules that possess different degrees of rigidity namely: poly (L-lysine) (PLL) dendrimer, ubiquitin, β-casein and α-synuclein from 190-350K. We show that the PLL dendrimer varies with temperature consistent with collision theory, and conclude, as expected, its structure does not alter significantly over this range. By contrast, the structure of each protein is altered by the temperature of the drift gas, with notable unfolding to all charge states at 350 K and also at 250 K, following predicted *in vitro* stability curves, and with conformational variation that gives qualitative insights to the effect of temperature on the free energy landscape of these proteins. We also show that we can kinetically trap unfolding intermediates at drift temperatures of 210 K and 190 K on a millisecond experimental time scale. For alpha-synuclein, the 13+ ions present two distinct conformers and VT-IM-MS measurements allow us to calculate the transition rate and activation energies for conversion between these. These data exemplify the capability of VT-IM-MS to provide insights to thermodynamics involved in conformational restructuring.

Introduction

Ion mobility spectrometry coupled with mass spectrometry (IMMS) has been widely used in the characterization of molecular conformation. In one single experiment, it is possible to obtain, chemical identity and complex stoichiometry from *m/z* values and conformational information in the form of a collision cross section (CCS)[1–4]. Ions are created and injected into a cell which contains an inert buffer gas. These ions are propelled through the cell under the influence of weak electric field and their arrival time at a detector is determined by their mass and charge as well as by the frequency and nature of the collisions that each ion makes with the gas. Mason and Schamp[5] related the average arrival time of ions to their rotationally averaged temperature dependent CCS using a first approximation of the ion transport equations. Consequently, the CCS is a composite parameter that is due to the ion, the buffer gas and the temperature of the gas. With commercially available IM-MS instruments it is not possible to directly explore the effect of temperature on CCS values, although the dependence has been noted and in pioneering experiments over 20 years ago, Bowers showed that that experimental CCS values of macromolecules were indeed temperature dependent in mobility measurements[6], illustrating this with the use of C_{60}^+ and observing that as the temperature decreases the CCS increases. This is attributable to the importance of the long-range interaction potential between the buffer gas and the analyte ion at low temperatures. As the buffer gas approaches the ion the trajectory of interaction is more affected by the long-range attraction resulting in a greater CCS value at lower temperatures. At high temperatures the buffer gas analyte interactions become more hard sphere like, and the CCS approaches a value that is less influenced by interatomic interactions. Such behaviour is evident from the collision theory developed by Mason and Schamp informed in turn with experiments on atomic and diatomic ions (equation [1]).[5] This behaviour can be predicted for rigid systems for which the resolution of IM measurements is inversely proportional to the square root of the temperature [5].

$$\Omega = \frac{3}{16}\frac{qE}{N}\sqrt{\frac{2\pi}{\mu k_B T}}\frac{1}{\overline{v_d}} \qquad [1]$$

In equation [1], ***N*** represents the number density of the drift gas, ***q*** denotes the charge of the ion, ***E*** is electric field, k_B is the Boltzmann constant, μ is the reduced mass of the ion of interest and the buffer gas; ***T*** is the gas

temperature and $\overline{v_d}$ is the average drift velocity[7]. Each variable in this equation plays a pivotal role in determining the CCS, allowing for a precise and comprehensive understanding of ion interactions within the drift gas environment[8].

Proteins are not rigid systems, and *in vitro* and *in vivo*, functional forms of proteins are influenced by a variety of factors[9], including temperature[10]. For eukaryotic proteins, their fold follows a stability curve, where in, they are most stable at physiologically relevant conditions and deviations from this to lower or higher temperatures induce denaturing and loss of the functional form[7]. Making experimental measurements that explore the effect of elevated temperature on protein structure is straightforward with a number of different methods available including isothermal calorimetry[11], NMR[12] and temperature jump spectroscopy[13] as well as mass spectrometry based proteomic methods such as LOPIT[14]. These have led to a body of work that agrees that increased thermal energy overcomes the energy required for non-covalent interactions to hold a protein in its folded state[8,15]. Such measurements have also been used to support two state unfolding models for structured proteins and the absence of such for Intrinsically Disordered Proteins (IDPs). By contrast, exploring the effect of low temperatures on destabilising protein structure, or on IDPs is nontrivial and much of the work in this area is theoretical, based on extrapolation from measurements made close to 273K[16] or with protic organic solvents which freeze at lower temperatures. The prevailing view from these studies is that as the aqueous environment around a protein freezes, it becomes more hydrophobic, which reduces the often-small stabilising influence of solvent interactions for the fold and causes the protein to denature[17].

It is well known that collisions in the gas phase can be used to alter the structure of proteins to gain insights to their topology and interactions, and IM-MS has been employed to examine unfolding and restructuring as well as dissociation. It is possible to estimate the temperature of the ion due to collisional interactions. VT IM-MS measurements also allow us to probe protein unfolding as well as monitor the effect of elevated temperature on conformational dynamics over 2-50 ms.

It is also possible to change the temperature of the ESI solution and use IM-MS to examine how conformations are altered from this[18,19]. The effect of low temperature on protein conformations in the gas phase has been less studied, in part due to the complex engineering requirements of such instrument, yet it provides a unique

environment for study. Russell and co-workers used cryogenic IM-MS to examine the conformational changes that occur during the hydration of a small peptide, one water molecule at a time. By varying the time ions spend in the drift cell, it is also possible to make thermodynamic measurements, and monitor the rate of conformer interconversion, which has been shown for peptides and disaccharides[20]. A typical VT-IM-MS workflow is shown in Figure 1, imposed onto a quadrupole time-of-flight IM-MS instrument as we adopt here. Changes to the temperature of the analyte can be made at different stages of the instrument. These include altering the temperature of the ESI source and hence the analyte solution[18] increasing the voltages in the desolvation optics to induce in source collisional activation[21]. More commonly, activation is performed on desolvated ions prior to the drift region in ion transfer optics or collision cells. In many IM-MS instruments it's also possible to increase the energy at which ions are injected into the drift cell, and finally some instruments permit the use of cooled drift gases down to cryogenic temperatures[22,23].

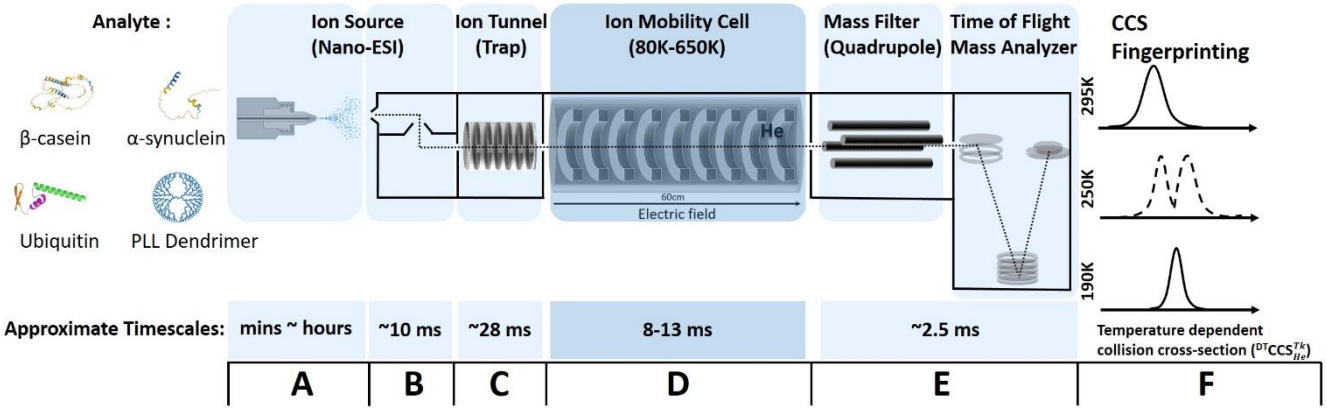

Figure 1: Schematic workflow of possible VT-IM-MS experiments and the approximate time spent by ions in each stage in our instrument for the four analytes under investigation. The structures of β-casein and α-synuclein are represented using alpha-fold[24], the 'A' state of ubiquitin is adapted from Brutscher et al.[25,26] and the dendrimer is a schematic representation of the structure, see below for more details. : A) Sample from solution phase is placed in a nano-spray capillary, which can be heated for mins to hours[27]. B) The time for an analyte to desolvate from the ESI droplet is 0.1~10ms[28]. C) Applying higher voltages in the source and transfer ion optics permits ion activation and ions are then trapped for ~28ms and released to ion mobility cell of length 50.5 cm in a 100 us packet using gating voltages. In our instrument the temperature of ions in the trap is ~295K even when the drift T is 150K[29] D) The drift time of ions is dependent on their mobility and the drift voltage and

in this instrument for the proteins of interest ranges from 8-13ms. Using cooling gases or heaters the temperature of gas in the drift cell can be altered from cryogenic to elevated temperatures and monitored with platinum resistance thermocouples in the cell. E) Ions are transferred via a quadrupole ion filter into a time of flight (ToF) mass analyser all at ~295K. F) Ions are detected in the form of mass resolved arrival time distributions, which are converted to temperature dependent collision cross-section ($^{DT}CCS_{He}^{TK}$). This instrument can be used to examine the effect of temperature on an ion's mobility as well as on its structure. Approximate timescales based on values that are typical in the instrument used here for ubiquitin.

Using VT IM-MS coupled with native IM-MS methods where a series of model structured proteins are infused from a salty solution that preserves the solution fold, we intriguingly found that an increase in the CCS at 260K indicating that the proteins will denature at low temperatures in the absence of solvent[30]. Using a higher resolution IM-MS instrument, we found that ubiquitin does not behave in this way, but rather more like a rigid system, however, following in source activation prior to injection to the drift cell we could capture unfolded intermediates with the use of low drift gas temperatures[23]. We have explored this effect further with monoclonal antibodies[31], where the role of low temperature has implications for the storage of biopharmaceuticals. Again, we found that these proteins extend at 260K and that this restructuring was more pronounced for mAbs where the hinge was stiffer (IgG2 vs. IgG4)[32]. This remarkable finding caused us to consider what happened to inter or intra molecular interactions as a function of changes in temperature. We postulate that the hydrogen bonds involved in non-covalent interactions in the native structures lengthen and weaken as the protein cools, the residual energy at 250-275K is sufficient to overcome the stabilisation they provide permitting restructuring.

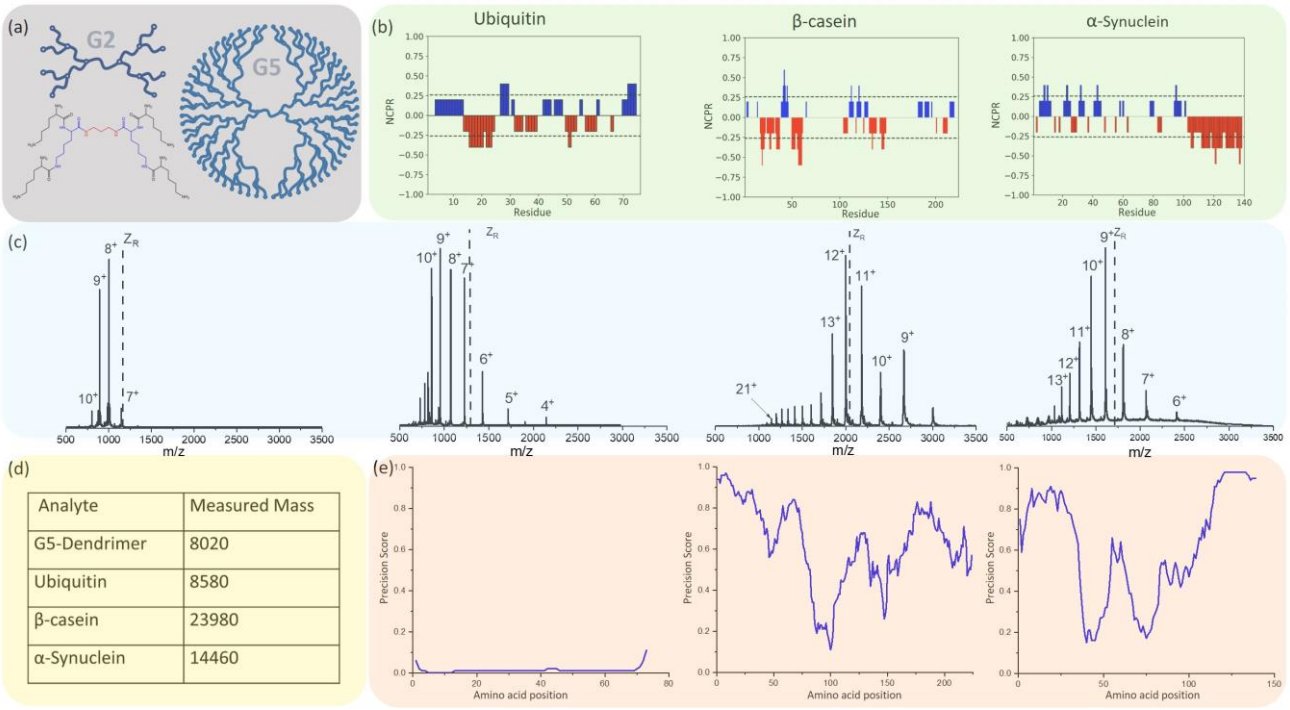

Analyte	Measured Mass
G5-Dendrimer	8020
Ubiquitin	8580
β-casein	23980
α-Synuclein	14460

Figure 2: (a) Chemical structure of the G2 PLL dendrimer with the core (red), as well as the constituents of G1 (blue) and G2 (black) and schematic structures of G2 and G5 (b) Net charge per residue (NCPR) profiles of construct along the linear sequence, adapted by CIDER[33]. (c) Typical mass spectrum of G5 PLL dendrimers from water, denatured ubiquitin sprayed from water: MeOH=1:1, PH-2.0; α-Synuclein and β-casein sprayed from 50mM ammonium acetate at T=295K, 20 μM, on the VT-IMMS instrument. The black dash line Z_R is the solution of an empirical relationship derived by De la Mora over the mass range of our test set of proteins, which describes the limit to the maximum charge that a spherical protein can hold[34]. (d) Measured mass of analytes. (e) DISOPRED plot for ubiquitin, α-Synuclein and β-casein[35].

IM-MS is highly suited to study conformational populations of intrinsically disordered proteins, that commonly present to the mass spectrometer with wide CCS and wide charge state distributions compared to more structured proteins[36,37]. Here, we examine the relevance of VT IM-MS applied to study conformational dynamic proteins using as exemplar systems, denatured ubiquitin, β-casein and α-synuclein (Figure 1, 2). We contrast their behaviours with that shown by a model polymer to allow us to decouple the effects of temperature on protein structure from the nature of the measurement. The structure of ubiquitin has been well studied with IM-MS[38–42]; and we have shown that for its low native like charge states, its CCS increases

with decreasing temperature in a similar way to C_{60}[23]. By contrast, β-casein and α-synuclein are highly disordered with most of their sequences lacking stable secondary or tertiary structure (Figure 2e)[43,44]. Whilst we have selected these compounds as demonstrators for the benefit of using VT IM-MS each has an important biological or biotechnological role. The G5 dendrimer is an example of a class of molecule that has been developed for drug delivery with high biocompatibility[45]; ubiquitin is a small regulatory protein found in most tissues of eukaryotic organisms[46], Its structure has been well studied by various techniques such as NMR and IM-MS[25,41]; β-casein is a major protein in milk that plays a crucial role in nutrient delivery and has high levels of disorder and conformational variability in lipid environments[47]; α-synuclein is a protein primarily involved in the regulation of synaptic vesicle trafficking and neurotransmitter release in the brain, it is implicated in the progression of Parkinson's disease[48]. For the proteins examined each has a different arrangement of charged residues which are differently segregated and for β-casein and α-synuclein (Figure 2b), as for other IDPs this is a signature of their high disorder[49–51] which can be distinguished readily with IM-MS. We chose the G5 poly (L-lysine) (PLL) dendrimer (Figure 2a) to compare the behaviour of these proteins to, since we have previously shown this family of dendritic polymers, possess stable and rigid conformations and G5 is a similar mass (8.02 kDa.) to ubiquitin (8.58 kDa.)

Methods

Sample preparation. A poly (L-lysine) (PLL) dendrimer of 5th generation was provided by AstraZeneca. Ubiquitin and β-casein were purchased from Sigma Aldrich, UK. Human recombinant α-synuclein was a gift from Rajiv Bhat, Jawaharlal Nehru University. expressed in BL21 (DE3) Escherichia coli and purified[52]. Ammonium acetate was purchased from Fisher Scientific (Loughborough, U.K.). Final protein concentrations were prepared to 20 µM β-Casein, 20 µM α-synuclein in 50 mM ammonium acetate, pH 6.8. Ubiquitin was prepared in H_2O: Methanol: formic acid = 49:49:2, pH 3.0. Stock solutions for each sample are stored in a -80°C freezer and are thawed 2 hours before each experiment. In our earlier exploratory study of α-synuclein we used a higher concentration and less stringent conditions regarding sample storage prior to analysis[23]. Representative mass spectra for each analyte are presented in the Figure 2c, along with biophysical data and

predicted mass for each protein, the value for the amount of net charge that could be supported on the surface of the isolated protein if it was globular[34]. Supplementary information Figure S1 represents the sequence, the Kappa value (κ) in supplementary information Table S1 gives an indication of the segregation of charge[50,53].

Variable Temperature Ion Mobility Mass Spectrometry We employed a home built instrument, which can be operated over 120-520 K obtain all measurements[29]. The configuration of this instrument and the methodology applied to obtain measurements as a function of different drift gas temperatures has been described in detail previously[23,29,32]. In brief: samples are loaded into fused silica nano-ESI capillaries (World Precision Instruments) into which is inserted a platinum wire (Goodfellow). These tips are loaded into the z-spray source of the mass spectrometer, equipped with a sampling cone interface, and the analyte ions are subsequently guided through two stacked ring RF guides to a trapping region prior to the drift tube. The drift tube consists of a series of electrodes, over which we can apply a field of 4.95-6.14 Vcm^{-1}. It is encased by a glass tube on the outside of which are heaters and a cooling coil.[29] The drift tube is filled with helium and its pressure is measured with a baratron (MKS instruments) and held constant to ± 0.02 Torr for each set of measurements. The drift cell is heated with wire wound ceramic heaters and cooled via the ingress of nitrogen gas through a serpentine copper coil that surround the drift region. This nitrogen gas is cooled by passing through a liquid nitrogen tank. For any given measurement the temperature is monitored on the outside with two K type thermocouples and with the drift cell with two PT100 thermometers. For each set of measurements, the temperature of the drift gas is maintained to ±2K. For each measurement the E/N ratio is maintained as low as possible to prevent alignment of the ions in the drift field and to ensure a similar number of collisions at each different temperature. Practically, the E/N values are all below 10.4 Townsends (Td.) which is far lower than that found in commercial IM-MS instruments and is significantly lower than k_bT ensuring that no field heating occurs and that ions are not aligned in the field during mobility separation[54,55]. The capillary voltage is typically held at 1.1-1.4 kV and the source temperature is set to 80°C. Inspection of the mass spectra at different temperatures (supplementary information Figure S2) indicates that cooling of the He buffer gas of temperature does not alter significantly the charge state distributions (CSD) of all analytes

examined. For each ion of interest, at each of the charge states it presents (Figure 2c), we record an arrival time distribution (ATD) which we convert to a CCS distribution, at T= 190, 210, 250, 275, 295 and 350 K.

Results

The Effect of Varying the Drift Gas Temperature on the CCS distributions

The IM-MS measurements for each of the analytes investigated show how this method can provide unique insights to their conformational preferences (Figure 3). For all species, at all charge states measured, the average $^{DT}CCS^{TK}_{He}$ value at T= 190 are larger than at 295 K as predicted by the kinetic theory of gases[20], in line with what we have previously reported for other proteins[23,32]. In order to best study the effect of temperature on restructuring the proteins, we highlight the behaviour of the charge state which is just above the value of z that could be supported on the surface of a globular protein[34]. These charge states are commonly more prone to unfolding/structuring from a globular form or native fold[34].

The temperature dependence in the arrival time distributions and collisional cross section distributions for each species is highly system dependent and, moreover, as the conformational diversity increases, G5<ubiquitin<β-casein<α-synuclein, the measured CCS distributions, even for single charge states, also become more complex. We observe trends in behaviour that locate each analyte on a continuum between intrinsically rigid and highly flexible. The G5-dendrimer (Figure 3a) behaves in a very similar fashion to that which has been previously reported for C_{60}, and in our prior work for native (low) charge states of ubiquitin, namely decreasing with temperature in accordance to eq. [1], inversely proportional to the square root of the temperature. The $^{DT}CCS^{TK}_{He}$/ Å^2 for $[M+8H]^{8+}$ increases by ~1.3% from 295K to 190K and slightly decreases from 295K to 350K. The mode $^{DT}CCS^{TK}_{He}$ of other charge states exhibit the same tendency as well (Supplementary data table S2).

The $[M+10H]^{10+}$ ion of ubiquitin (Figure 3b), behaves as predicted by Gabelica and Marklund for calculations performed using the A-state of Ubiquitin[56], with a steady increase in CCS as the drift gas temperature decreases suggesting only small structural perturbation, although at 350K there is evidence for some elongation suggesting the start of thermally activated unfolding[23,57]. Similar effects are observed for the other

charge states of denatured ubiquitin (Supplementary data table S3) as the drift gas temperature is lowered the CCS increases by 1.33 % for $[M+8H]^{8+}$ and 4.1% for $[M+11H]^{11+}$. In sub-ambient experiments, the mode $^{DT}CCS_{He}^{TK}$ of denatured ubiquitin in the higher charge state (z = 7-10) gradually increases with decreasing temperature as predicted according to equation [1][5,56,58,59](Supplementary data table S2). For $[M+10H]^{10+}$ ions the CCS is 1912 $Å^2$ at 295 K and rises to 2198 $Å^2$ at 190 K, corresponding to a relative increase of by 14.5%, which is above that predicted over this temperature range. For $[M+10H]^{10+}$ there are also some smaller lower populated conformers, which appear to be better resolved at lower temperatures as is the main species. At room temperature the CCS values of these are 1355 and 1676 $Å^2$ which correspond to intermediates in the interconversion between the N and A state as described previously[25,41]. The benefit of low temperature IM measurements is that we can freeze out these species. The CCS of any gas-phase ion depends on both the effective temperature of the ion and the ion-neutral interaction potential. At lower temperatures, the long-range attraction between the analyte ions and the buffer gas is more dominant, whereas at higher temperatures, the interactions become hard sphere like. This is beautifully exhibited by the behaviour of the G5 dendrimer, which exhibits a small decrease in CCS when the DT temperature is increased to 350 K, in line with kinetic theory (Equation [1]).

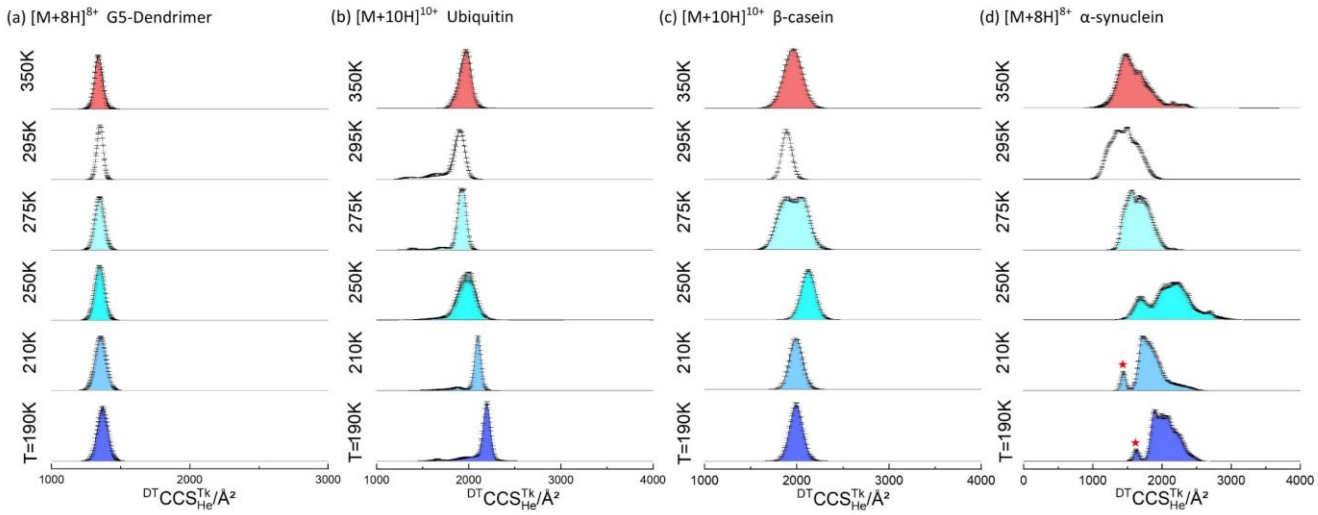

Figure 3: CCS distributions for the most representative ESI ions $^{DT}CCS_{He}^{TK}$ data is shown for measurements made at T= 295 K, 275 K, 250 K, 210 K and 190 K respectively for (a) [M+8H]8+ 5th generation PLL Dendrimer, (b)

$[M+10H]^{10+}$ ubiquitin (c) $[M+10H]^{10+}$ β-casein and (c) $[M+8H]^{8+}$ α-synuclein. Error bars represent the standard deviation from three replicates. We tried to maintain the E/N values within reason, and practically this was ~10 Td. for 350K, and ~5 Td. for 190K. Here is the interactive plot for data above.

Given that the G5-dendrimer exhibits such ideal behaviour as the temperature is varied, it is useful to contrast this with measurements for proteins, especially those that are more conformationally dynamic as it allows us to distinguish the physics of buffer gas ion interactions, from the effect of the temperature of the buffer gas on the structure of the molecule.

The disordered proteins β-Casein (Figure 3c) and α-synuclein (Figure 3d) present a different conformational landscape at every temperature. At 350K, both appear to start to thermally denature, as for $[M+10H]^{10+}$ ubiquitin. Unlike the G5-dendrimer, the $^{DT}CCS_{He}^{350K}$ of ubiquitin $[M+10H]^{10+}$ increases 5% at 350 K, and similar behaviour is apparent for β-casein and α-synuclein (Figure 3, 4, 5). As the drift temperature decreases, for $[M+10H]^{10+}$ β-Casein primarily retains its unimodal CCS distribution, except at 275 K (see below). Other charge states show more complex restructuring (Figure 4). The behaviour at 210 and 190 K is as predicted, although the increase in CCS compared to the value at 295 K varies. For example with $[M+10H]^{10+}$ it is 5%, whereas for $[M+16H]^{16+}$ it is 8.9%. With the high charge states of β-casein, (z>20) the net change in CCS between 295 K and 190 K is only ~1.5% which suggests that, like the dendrimer, these highly extended conformers are rigid forms that are primarily only influenced by the difference in buffer gas ion interactions at the lower temperature. α-synuclein shows far more complex behaviour with the change in drift gas temperature, as previously reported[23]. For the $[M+8H]^{8+}$ ion, at temperatures below 250K, a very distinct conformer with a CCS of 1445 $Å^2$ at 210K and 1632 $Å^2$ at 190K is revealed, this is not resolved at higher temperatures suggesting that it is preserved by cryo-freezing when injected into the cold drift cell, and that either it restructures to a more extended form when the drift gas temperature is 250K and above or it is not able to be resolved from the myriad of other conformers with higher CCS values for this charge state. If we compare the predicted maximum resolution R_{Max} for the dendrimer with the value from experiment, we find that the resolution does not increase as we lower the temperature. This apparent discrepancy is likely due to a number of closely related conformers that anneal at room temperature and start to separate at lower T (Supplementary

information Table S5). This said, the sharp conformers seen for both ubiquitin and α-synuclein are approaching R_{Max} at lower T. In summary, the IM measurements at temperatures below 250K show higher resolution than at room temperature, which exemplifies how such measurements may be useful to resolve low energy conformers. The majority of living organisms on earth, need to survive temperatures between 250 and 350K. Whilst it is possible with other biophysical method to explore the effects of temperatures at and above 275K the region from 250 -275 is far less tractable, our data highlights how IM-MS is able to probe this range.

The effect of drift cell temperatures from 250-275K on analyte structure.

The conformational behaviour of each of the proteins studied at 250 and 275 K is not solely attributable to the increased resolution at lower drift gas temperatures due to slower diffusion, nor the effects of buffer gas ion interaction (Figure 3). For Ubiquitin at 250 K, the measured $^{DT}CCSD_{He}^{250K}$ is significantly wider, indicating that some or all the conformers present at room temperature have restructured to larger forms. Such effects were not observed for the lower charge states of ubiquitin, more associated with the native fold[23] although we have previously reported similar behaviour for native charge states of intact and disulphide-reduced lysozyme, bovine pancreatic trypsin inhibitor (BPTI) and myoglobin[23,30].

For IDPs, this temperature-dependent change is also observed albeit with more complicated CCS distributions: take $[M+10]^{10+}$ of β-casein (Figure 3c) as an example, the mode of the $^{DT}CCSD_{He}^{295K}$ measured at 295 K in this experiment is 1894 $Å^2$ which is consistent with previous published data[60]. When the temperature drops to 275 K, the $^{DT}CCSD_{He}^{275K}$ now comprises two species of similar intensity, one (1938 $Å^2$) which is 2% greater than the value at 295 K and a second conformer at ~ 2000 $Å^2$. We infer from this that approximately half of the population of ions present now have restructured to a more extended conformer. At 250 K, the $^{DT}CCSD_{He}^{250K}$ of casein is again unimodal, and now centred at 2050 $Å^2$, an increase of 8.% compared to $^{DT}CCS_{He}^{295K}$, a far greater increase than shown by the G5 dendrimer, implying that at this temperature all conformers elongate. We interpret this behaviour as cold denaturation of the protein in a gaseous environment. The other dominant charge states of β-casein behave in a similar fashion (Figure 4) although the magnitude of the increase at 250 K is lesser for higher charge states.

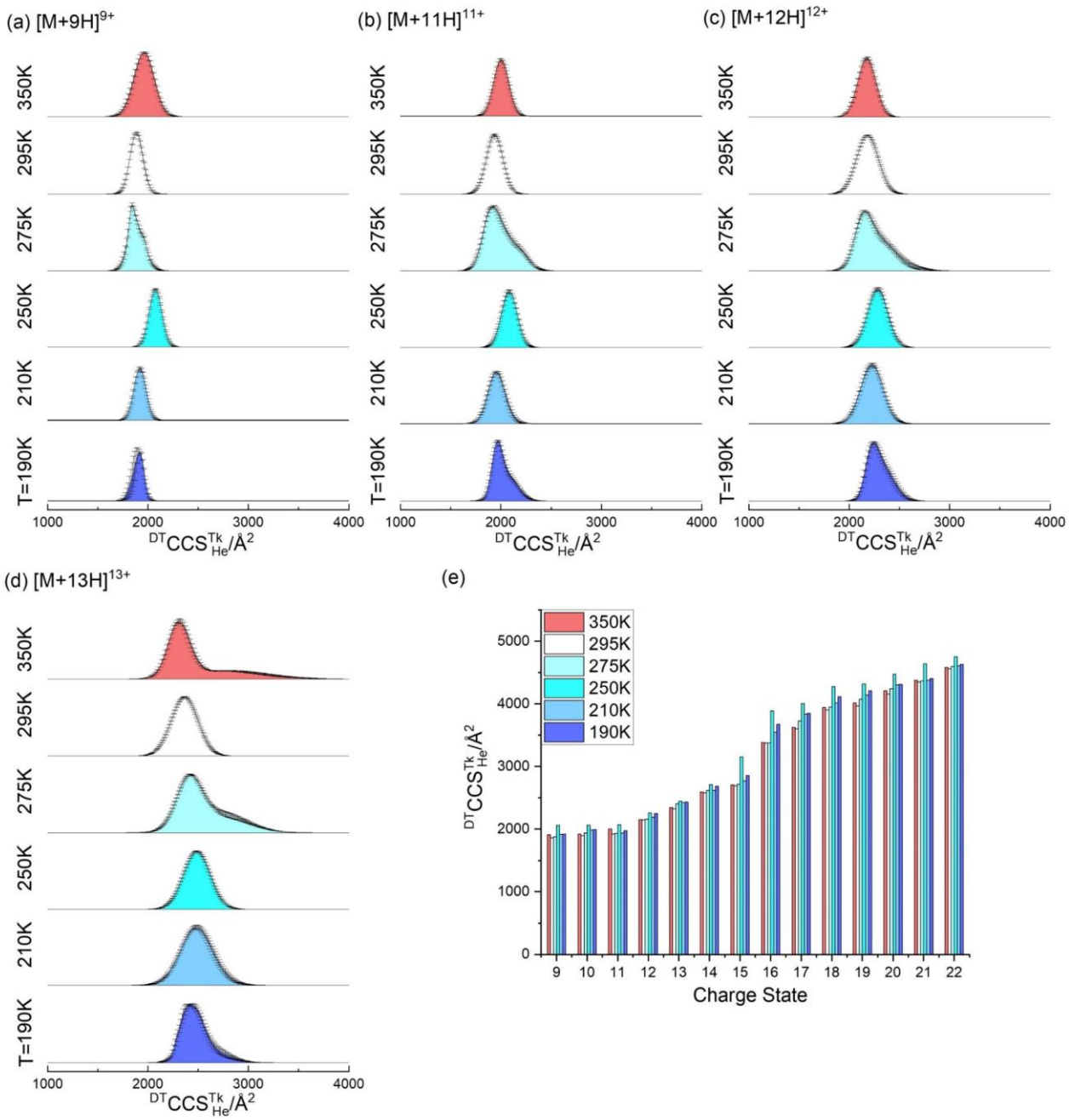

Figure 4: β-casein Collision cross section distributions ($^{DT}CCS^{TK}_{He}$) for the four most abundant ions: (a) $[M+9H]^{9+}$, (b) $[M+11H]^{11+}$, (c) $[M+12H]^{12+}$ and (d) $[M+13H]^{13+}$ in the temperature range of 295 K to 190 K. Error bars represent the standard deviation from three replicates. Sub-ambient temperature median $^{DT}CCS^{TK}_{He}$ value for all other detected charge ($[M+9H]^{9+}$ - $[M+22H]^{22+}$) states are shown in (e). Here is the interactive plot for data above.

For β-casein, the increase in the average $^{DT}CCS^{250K}_{He}$ of $[M+9H]^{9+}$, $[M+10H]^{10+}$, and $[M+11H]^{11+}$ are 10.7%, 8.2%, and 7.7% whereas for $^{DT}CCS^{250K}_{He}$ of $[M+21H]^{21+}$ and $[M+22H]^{22+}$ the increase is only 2.1% and 4.0%. We speculate

that this may be related the number of stabilising non-covalent interactions that an ion at a given charge state has as it enters the cold drift cell. For low charge states we have previously postulated that the H-bonds which stabilise more compact conformers, extend as the temperature of the ion decreases. At temperatures between 250-275 K there is sufficient residual energy in the protein that this lengthening of H-bonds leads to the decoupling of regions that are connected with these H-bonds. The higher the charge state the fewer of such interactions exist as they have already been reduced by coulombic repulsion due to proximal protons, and the less perturbation to these can occur. To investigate this behaviour further, we performed experiments which couple collision induced activation with IM measurements (aIMS) on β-casein, (Supplementary information Figure S5) which show similar effects. The lower charge states restructure via stable intermediates, presumably due to stabilising non-covalent interactions, requiring more collisional energy to fully extend, whereas higher charge states restructure with far less energy and via less stable intermediates, indicating that coulombic effects are the main driver.

NCPR and disorder predictions (Figure 2b, 2e) indicate that α-synuclein may have relatively higher conformational diversity than β-casein, since the opportunity to form many different stabilising interactions is provided by segregated patches of oppositely charged amino acids. This hypothesis is supported as well by ambient temperature experiments where the CCS distributions for the low charge states $[M+7H]^{7+}$and $[M+8H]^{8+}$ are broad (Supplementary information Figure S4). For higher charge states ranging from $[M+10H]^{10+}$ to $[M+13H]^{13+}$, two or three distinct conformations are observed at room temperature. In this study these are better resolved than in our previous exploratory reports[23,29,32] and the data here is highly reproducible which we attribute to more careful sample preparation which reduced the contribution from counter ions on the protein as well as lowered the potential for conformers that are dissociated from higher order aggregates.

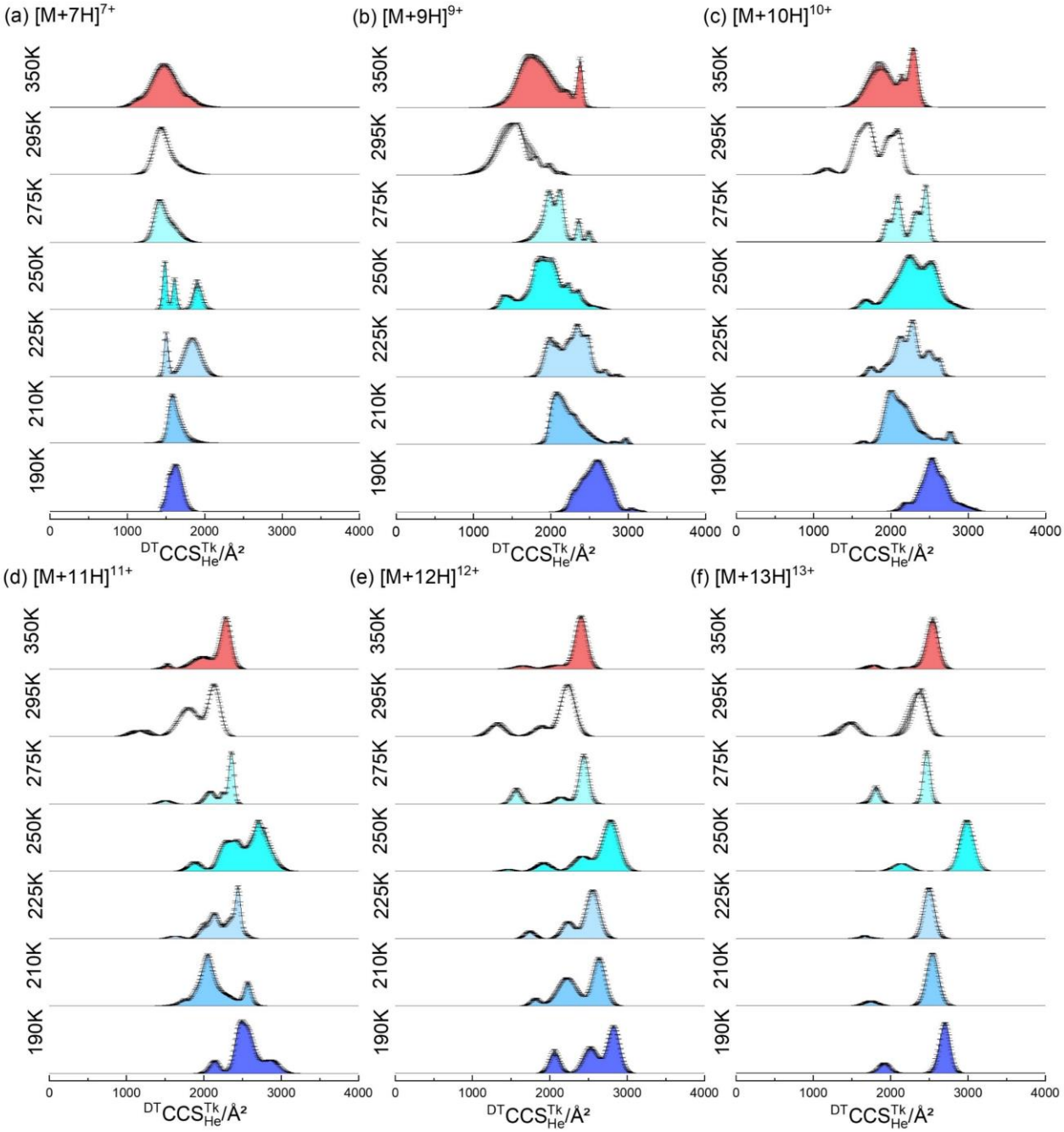

Figure 5: α-synuclein Collision cross section distributions ($^{DT}CCS^{TK}_{He}$) for (a) $[M+7H]^{7+}$, (b) $[M+8H]^{8+}$, (c) $[M+9H]^{9+}$, (d) $[M+10H]^{10+}$, (e) $[M+11H]^{11+}$, (f) $[M+12H]^{12+}$, in the temperature range of 295 K to 190 K; Error bars represent the standard deviation from three replicates. Here is the interactive plot for data above.

For all charge states of α-synuclein, significant restructuring occurs at T=250 K, for the intermediate charge states z= 9, 10 and 11, this is also evident at T= 275 K. For $[M+8H]^{8+}$ at T=250, the average $^{DT}CCS^{250K}_{He}$ increases by 44% from 1510 Å^2 at 295 K to 2180 Å^2, *cf*. β-casein where, as discussed above, the increase ranges from

2% and 17% (Supplementary information Table S4). This behaviour contrasts with $[M+7H]^{7+}$, which behaves more akin to ubiquitin in lower charge states, with less evidence of global restructuring and CCS distributions that alter mostly due to ion mobility effects, indicating that the conformers at this charge state have many stabilising non covalent interactions. At 275 K for $[M+11H]^{11+}$ and higher charge states, the $^{DT}CCS_{He}^{275K}$ are better resolved, with the apex $^{DT}CCS_{He}^{275K}$ increased more than for the dendrimer at this temperature, indicating restructuring to more distinct conformers.

For $[M+7H]^{7+}$ and $[M+8H]^{8+}$, such changes at T= 250 K are far less significant, but still evident. For the most abundant intermediate charge states (9+ and 10+) at T =250 K, there are now conformers which have a median $^{DT}CCS_{He}^{250K}$ increase of 33% and 25%, respectively. Whilst this behaviour is similar to that shown by β-casein, the magnitude of the restructuring to larger conformers is greater.

For α-synuclein we carried out additional measurements at 225 K to determine if the conformational changes seen at 250 K are unique to that temperature. For the high charge state ions (z=10 to 13) the $^{DT}CCS_{He}^{225K}$ distributions are very similar to those at 275 K with the slight increase in CCS magnitude expected at this temperature. The width of the conformers at 225 K is surprisingly wider than at 275 K and there is some evidence for conformers that are not resolved at higher temperatures, starting to be distinguished, most evident for z =10 and 11. Ions with z<10 also exhibit a larger than expected increase in CCS at 225 K. The same effect is most pronounced for $[M+9H]^{9+}$ and $[M+10]^{10+}$, which possess very similar $^{DT}CCS_{He}^{225K}$ distributions as for $^{DT}CCS_{He}^{275K}$. This suggests a wider temperature range over which the low temperature denaturation can occur to initially compact ions.

In the lowest temperature experiments (210 K and 190 K), $[M+7H]^{7+}$ exhibited similar features as those of β-casein and other structurally rigid analytes: the median $^{DT}CCS_{He}^{TK}$ was slightly higher than at ambient temperature and the $^{DT}CCS_{He}^{TK}$ range was slightly narrowed. But for $[M+8H]^{8+}$ (Figure 3d), we captured one additional frozen compact conformational population (denoted by an asterisk * in Figure 3d) at 250 K, 210 K and 190 K. This new compact species (*) is not resolved at higher temperatures, indicating that it arises from a smaller conformer that unfolds at higher temperatures. The rate of this conformational transition must be much higher at higher temperatures, with a lower activation barrier, and must occur to completion during the

thermalisation in the first few mm of the drift cell, explaining the absence of this structure, during those experiments. There is no overlap between this kinetically trapped compact conformation and the restructured conformational ensembles at 250 and 275K. The $[M+9H]^{9+}$, $[M+10H]^{10+}$ and $[M+11H]^{11+}$, (Figure 5) also exhibit more complex changes at 210 and 190K. They are highly dynamic and have a broad conformational landscape at 295 K, which resolves to very distinct conformers at 275K suggesting that the interconversion rate decreases with temperature and states that are freely interconverting at higher temperatures become kinetically trapped. At 250K these distinct conformers now disappear and as for β-casein there is substantial restructuring to extended highly overlapped conformers. In summary, the high charge state α-synuclein ions only cold restructure at 250K and are conformationally trapped at 275K and below 250K. To further investigate the behaviour of α-synuclein, at 250 K we performed in source activation, by increasing the cone voltage from 40V to 90V prior to IM-MS measurements (Supplementary information Figure S7). Whilst we see a slight increase in the overall CCS values for the conformational distributions it is far less, especially for the lower charge states than observed at 295 K, indicating that the cold restructuring is taking each conformational ensemble to its most extended state. For each of the charge states at 250K there is conformational occupancy just under 3000 $Å^2$, which is also occupied by the activated conformers at 295K. Remarkably the theoretical CCS limit for the linear sequence is 3880 $Å^2$ which suggests that cold activated or in source activated still leaves conformers with some structural elements held rigid by non-covalent interactions, for example helices. The effect of cold restructuring on α-synuclein is of a similar magnitude to than achieved in CIU experiments at ambient temperature. Take the case of $[M+8H]^{8+}$ as an example; when the activation energy reaches 600eV, the ${}^{TW}CCS^{295K}_{N2\rightarrow He}$ is ~ 2200 $Å^2$, similar to the non-activated ${}^{DT}CCS^{250K}_{He}$ at 250K. By contrast, the unfolding of β-casein observed at 250K is less than the unfolding with 600eV in the collisional activation experiment. In comparison, as we have previously shown, low charge states of ubiquitin unfolds at 600eV in aIMS but exhibit no significant structural rearrangement during IM-MS measurements at 250K[23] . These observations exemplify the sequence dependence cold denaturation even when applied to IDPs.

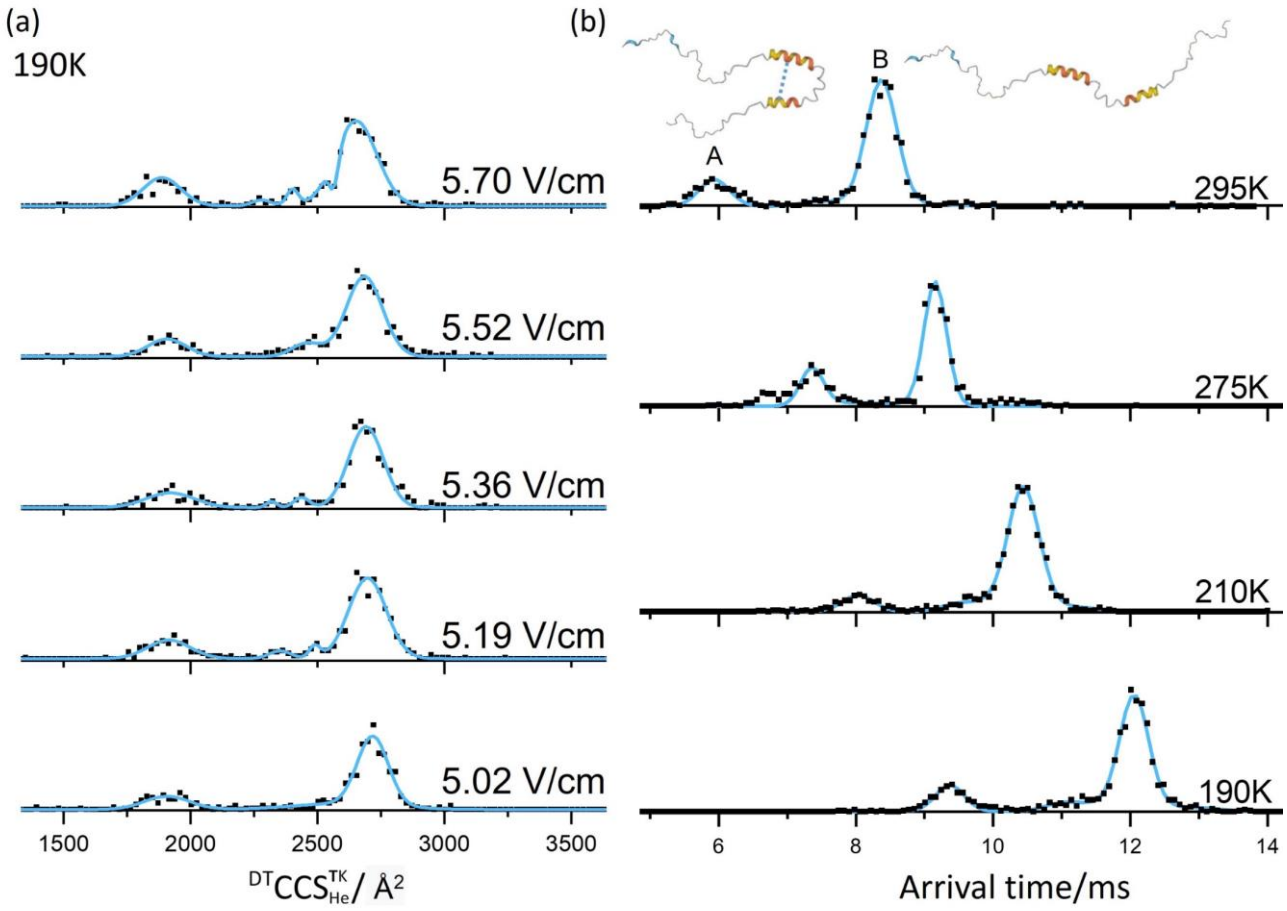

Figure 6: Sub-ambient temperature $^{DT}CCSD_{He}^{190K}$ and ATD of α-synuclein $[M+13H]^{13+}$. (a) Fitted $^{DT}CCSD_{He}^{190K}$ (blue line) and experimental value (black dots) at 5 drift voltages, in decreasing order, at 190 K. (b) Interconversion rate constant calculation simulation fitted to the ATDs obtained at the lowest drift voltage for which reasonable signal was obtained at: 295 K, 275 K, 210 K, 190 K from top to bottom. Black dots represent experimental values, and blue solid lines represent Simulated ATD. The hypothetic schematic of the α-synuclein structure is adapted from AlphaFold Protein Structure Database[61].

Conformational dynamics of α-synuclein captured in real-time: experimental measurement of conformational transition rate constants

The $^{DT}CCSD_{He}^{295K}$ of $[M+13H]^{13+}$ ions of α-synuclein at 295 K have two highly distinguished conformations (Figure 6a, Figure 5f) with ATDs that also show ion density between these two species over the temperature range examined, a behaviour that is characteristic of gas-phase reactions[57]. Since we are examining monomeric molecular cations, and we have excluded other sources of such ions, such as dissociating multimeric states,

the observed behaviour can be attributed to gas-phase conformational dynamics. From this exemplary dataset we apply a curve-fitting method, modelling the reaction-diffusion-advection phenomena in the drift tube experiment, to obtain kinetic rate constants for those transitions directly by analysing the arrival time distributions and fitting them with a reaction-advection-diffusion model using two reacting species (a similar method has been employed by Poyer et al[62]). Since the initial and final states are not baseline separated, the conformational transition is not driven to an equilibrium state, where the species would appear as a single peak between the two. When the temperature is lowered to 190 K (Figure 5a), the rate constant is reduced further, slowing down the reaction. When the drift voltage gradually decreases from 5.70 Vcm^{-1} to 5.02 Vcm^{-1}, which corresponds to longer drift times, the abundance of compact conformation A decreases. In the first four voltages, we captured some intermediate states between conformations A and B. When the drift voltage reached 5.02 Vcm^{-1}, the intermediate states are not abundant, and the content of A reached the lowest value among the five groups of voltages. At longer times the process tends more towards an equilibrium state. Similar conditions were not captured for other charge states. Average rate constants from A to B at 295 K, 275 K, 210 K, and 190 K are 0.69 s^{-1}, 0.63 s^{-1}, 0.50 s^{-1}, and 0.47 s^{-1} respectively, which follow an Arrhenius relationship (Supplementary information Figure S9), bolstering the viability of the curve fitting. The activation energy, assuming a three-state model, is at 1.79±0.12 kJ/mol from A to B. Intriguingly this activation energy is far lower than expected transitions; and is only equivalent to the formation or breaking of one hydrogen bond. We can speculate on what conformers could have such a small energy difference.

Martin F. Jarrold and co-workers have reported the unfolding of an desolvated helix upon experiencing a similar temperature change[57], with a rate constant for this of 243 s^{-1}. There is ample evidence for preservation of helical proteins and helices in vacuo, and we have previously reported that some peptides will form helices upon transfer to the gas phase[63]. There is also evidence that α-synuclein has a helical forming propensity[64,65], which is supported by alpha-fold predictions (Figure 7) albeit only in a few regions or induced by TFE[66], and so likely only transient in aqueous environments for this highly disordered protein; in-cell NMR has not revealed any evidence for substantial helicity[67]. It has been suggested that α-synuclein may form a more stable helical structure in a highly hydrophobic environment[65,68,69]. Given that the gas phase is the ultimate hydrophobic

environment, we speculate that both conformers may contain helix regions formed or captured upon desolvation, and that these have formed a helix-helix interaction (early arriving conformer) which is stabilised by 1 or 2 inter helix H bonds, which break to 'pop' a hair pin to a more extended form (Figure 6b). A β-hairpin that constrains some transient helical regions has been postulated by MD simulations[70], and metal ions and the molecular tweezer CLR01 have been shown to dramatically alter the conformational landscape of α-synuclein[71]. These studies along with the finding here are all indicative that distal regions of this protein can be held together by small interfaces in the apo form, that when disrupted cause a large conformational change. The observation that these configurations survive even at 350 K, indicates that both possess some inherent stability as would be imparted by secondary structural elements.

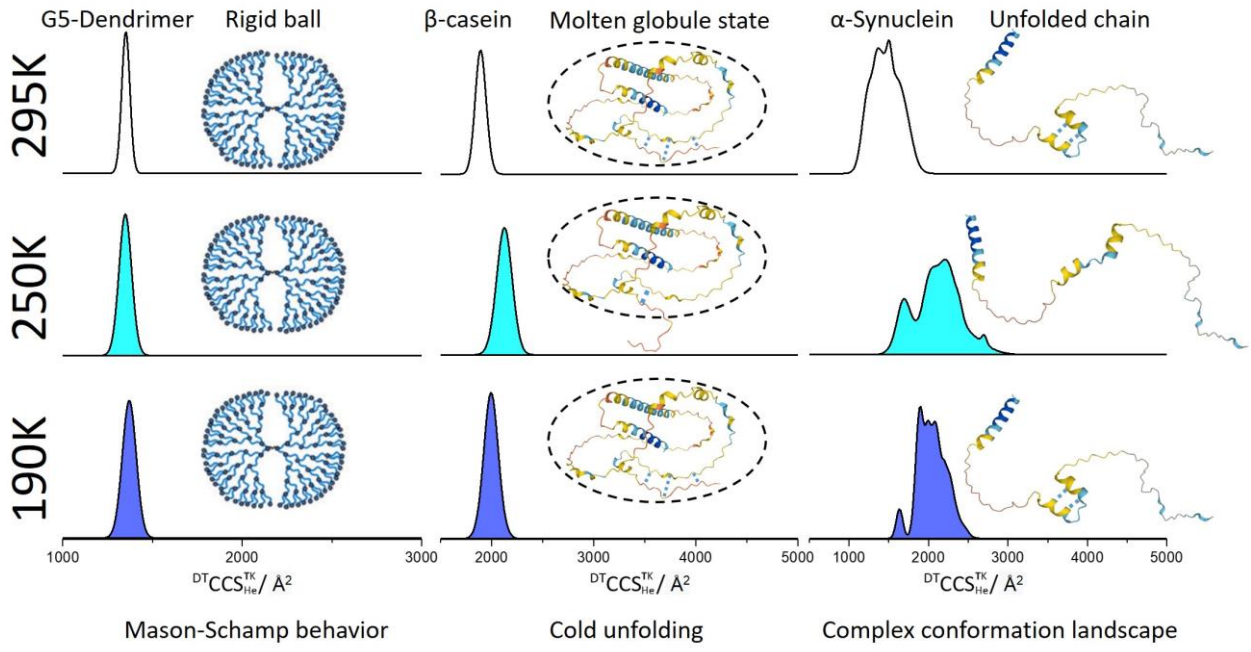

Figure 7: Summary of the effect of drift gas temperature on the conformational landscapes of the G5-dendrimer, β-casein and α-synuclein. The blue dotted lines represent possible stabilising hydrogen bonds that are disrupted at temperatures around 250K. At each of the experimental temperatures of 295K, 250K, and 190K, each charge state of the G5-Dendrimer structure is globular and does not restructure, and this model system behaves as predicted by Mason-Schamp[5]. β-casein mostly also only presents one conformer per charge state, which probably are molten globule states, stabilised by many noncovalent interactions, at 250 K hydrogen bonds are lengthened and the protein ion still has residual energy, so these stabilising interactions

are disrupted. α-synuclein has a far more complex conformational landscape even within each charge state, which may be part explained by transient helical regions stabilised in the gas phase. Any hydrogen bonds will also lengthen and potentially break at 250K.

Conclusions

Variable-temperature ion mobility spectrometry has allowed us to map out the conformational landscapes of three different proteins and contrast the behaviour of these with that of a synthetic G5 PLL dendrimer. For the proteins we studied, VT IM-MS showed directly that in addition to a temperature dependent glass transition in polypeptides, cold denaturation is accompanied by marked conformational changes. These effects are not present in the rigid G5 PLL dendrimer and become more pronounced in intrinsically disordered proteins. Figure 7 summarises the major differences between the effects of making VT IM-MS measurements on the rigid dendrimer and on the IDPs. For the dendrimer (Figure 7a) the behaviour is as predicted by ion transport theory, and the increase in CCS as the temperature decreases does not indicate any restructuring of the analyte. This is similar to the effect of taking measurements at lower drift gas temperatures for the native charge states of the highly structured protein ubiquitin and as such we can surmise that when complexes are rigid and held by many stabilising non-covalent interactions they will not alter shape substantially in the ~ 5-20 ms time spent in the cold drift gas. The higher charge states of ubiquitin as reported here, do appear to alter in conformation at 250 K, and this indicates that the fewer number of stabilising non covalent contacts are not sufficient to hold the more extended structure together at a temperature when the H-bond lengthen and there is still enough residual energy in the analyte to allow these to break. Previously, we have shown similar restructuring at lower drift gas temperatures for BTPI, cytochrome c myoglobin at 260 K and lysozyme and IgGs at 250 K[30,32]. For lysozyme, the CCS increase at this temperature is greater in its disulfide reduced form, which also underlines the importance of stabilising interactions and the subtle way the conformational stability can be altered at sub ambient temperatures.[23]

For IDPs and denatured forms of ubiquitin, varying the temperature at which the IM measurements provides insights to the low barriers for interconversion between conformers for these conformational dynamic molecules. For β-casein, the protein is mostly only present as 1 or at the most 2 conformers per charge state,

and all of these extend at 250 K, particularly for the higher charge states. For α-synuclein the VT IM-MS measurements show a complex interplay between the ability of the measurement to resolve different conformers and how these are differently susceptible to restructuring between 225 and 275K.

From an energetic point of view, the unfolding behaviour at 250 K is the result of the competition between molecular kinetic energy and potential energy. At a certain temperature, the decrease in thermal motion is balanced by the increase in potential energy. The molecule requires a certain residual thermal energy to overcome the stabilising effects of the weakening H-bonds to restructure to a more extended conformation (Supplementary information Figure S8). At lower temperatures the extent of residual intramolecular motions, is lower and the freezing process is faster which means that the molecules appear to retain their ambient temperature conformations. The $^{DT}CCS^{TK}_{He}$ values obtained at 210 K and 190 K are consistently lower than those measured at 250 K. Comparing the two IDPs low-temperature data above, we are led to conclude that the energy barriers in the α-synuclein conformational energy landscape are lower and it is more able to extend. Comparatively, structured proteins have much higher energy barriers due to a greater number of intramolecular interactions, thus limiting the extent of structural change at 250K. Interestingly the magnitude of conformational change for α-synuclein at 250K is larger than that experienced in CIU experiments, for β-casein the opposite is observed. For the single example we show of the interconversion between a compact and an extended conformer of α-synuclein the energy barrier appears very small, which highlights the power of sub ambient IM-MS experiments in discerning the low energetic differences between the conformational landscapes of these disordered proteins.

Overall our experiments show how high-resolution IM-MS can separate and characterise the structures of conformational heterogeneous molecules, such as IDPs, which due to this heterogeneity cannot be characterised adequately by methods relying on bulk measurements.

Our experiments differentiate clearly between the behaviour of conformational dynamic proteins (IDPs and denatured forms) and more rigid due to covalent and non-covalent interactions. The distinct restructuring observed at drift gas temperatures close to 250K appears to be a universal property of eukaryotic proteins occurring at the temperature at which they are predicted to cold-denature[23,30,32]. Such insights, which are hard

to obtain with any other experimental method, are valuable for understanding the fundamental effect of temperature on protein stability which may also have more practical use to inform on the storage of proteins and critically to examine the effect of temperature on the proteins in plants and other food supplies as we experience the on-going climate emergency.

References

1. Jurneczko, E. & Barran, P. E. How useful is ion mobility mass spectrometry for structural biology? the relationship between protein crystal structures and their collision cross sections in the gas phase. *Analyst* **136**, 20–28 (2011).
2. Heck, A. J. R. Native mass spectrometry: A bridge between interactomics and structural biology. *Nature Methods* **5**, (2008).
3. Keppel, T. R., Howard, B. A. & Weis, D. D. Mapping unstructured regions and synergistic folding in intrinsically disordered proteins with amide H/D exchange mass spectrometry. *Biochemistry* **50**, (2011).
4. Testa, L., Brocca, S. & Grandori, R. Charge-surface correlation in electrospray ionization of folded and unfolded proteins. *Analytical Chemistry* **83**, (2011).
5. Mason, E. A. & Schamp, H. W. Mobility of gaseous lons in weak electric fields. *Annals of Physics* **4**, 233–270 (1958).
6. von Helden, G., Wyttenbach, T. & Bowers, M. T. Conformation of macromolecules in the gas phase: use of matrix-assisted laser desorption methods in ion chromatography. *Science* **267**, 1483–1485 (1995).
7. Bischof, J. C. & He, X. Thermal Stability of Proteins. *Annals of the New York Academy of Sciences* **1066**, 12–33 (2006).
8. Sun, P. D., Foster, C. E. & Boyington, J. C. Overview of Protein Structural and Functional Folds. *Current Protocols in Protein Science* **35**, 17.1.1-17.1.189 (2004).
9. Sanchez-Ruiz, J. M. Protein kinetic stability. *Biophysical Chemistry* **148**, 1–15 (2010).
10. White, R. H. Hydrolytic stability of biomolecules at high temperatures and its implication for life at 250 degrees C. *Nature* **310**, 430–432 (1984).

11. Schön, A., Clarkson, B. R., Jaime, M. & Freire, E. Temperature stability of proteins: Analysis of irreversible denaturation using isothermal calorimetry. *Proteins: Structure, Function, and Bioinformatics* **85**, 2009–2016 (2017).
12. Jung, A., Bamann, C., Kremer, W., Kalbitzer, H. R. & Brunner, E. High-temperature solution NMR structure of TmCsp. *Protein Science* **13**, 342–350 (2004).
13. Callender, R. & Dyer, R. B. Probing protein dynamics using temperature jump relaxation spectroscopy. *Current Opinion in Structural Biology* **12**, 628–633 (2002).
14. Dunkley, T. P. J., Watson, R., Griffin, J. L., Dupree, P. & Lilley, K. S. Localization of organelle proteins by isotope tagging (LOPIT). *Mol Cell Proteomics* **3**, 1128–1134 (2004).
15. Sansom, C., Walshaw, J. & Moss, D. Principles of protein structure. *Biochemical Society Transactions* **25**, 377S.5-377S (1997).
16. Privalov, P. L. Cold Denaturation of Protein. *Critical Reviews in Biochemistry and Molecular Biology* **25**, 281–306 (1990).
17. Dias, C. L. *et al.* The hydrophobic effect and its role in cold denaturation. *Cryobiology* **60**, 91–99 (2010).
18. Laganowsky, A., Clemmer, D. E. & Russell, D. H. Variable-Temperature Native Mass Spectrometry for Studies of Protein Folding, Stabilities, Assembly, and Molecular Interactions. *Annual Review of Biophysics* **51**, 63–77 (2022).
19. May, J. C. & Russell, D. H. A mass-selective variable-temperature drift tube ion mobility-mass spectrometer for temperature dependent ion mobility studies. *Journal of the American Society for Mass Spectrometry* **22**, 1134–1145 (2011).
20. Gidden, J. & Bowers, M. T. Gas-phase conformational and energetic properties of deprotonated dinucleotides. *Eur. Phys. J. D* **20**, 409–419 (2002).
21. Attygalle, A. B., Xia, H. & Pavlov, J. Influence of Ionization Source Conditions on the Gas-Phase Protomer Distribution of Anilinium and Related Cations. *J. Am. Soc. Mass Spectrom.* **28**, 1575–1586 (2017).
22. Camacho, I. S. *et al.* Native mass spectrometry reveals the conformational diversity of the UVR8 photoreceptor. *Proceedings of the National Academy of Sciences* **116**, 1116–1125 (2019).

23. Ujma, J. *et al.* Protein Unfolding in Freeze Frames: Intermediate States are Revealed by Variable-Temperature Ion Mobility–Mass Spectrometry. *Anal. Chem.* **94**, 12248–12255 (2022).
24. alpha synuclein in UniProtKB search (4574) | UniProt. https://www.uniprot.org/uniprotkb?query=alpha+synuclein.
25. Vajpai, N., Nisius, L., Wiktor, M. & Grzesiek, S. High-pressure NMR reveals close similarity between cold and alcohol protein denaturation in ubiquitin. *Proceedings of the National Academy of Sciences* **110**, E368–E376 (2013).
26. Brutscher, B., Brüschweiler, R. & Ernst, R. R. Backbone dynamics and structural characterization of the partially folded A state of ubiquitin by 1H, 13C, and 15N nuclear magnetic resonance spectroscopy. *Biochemistry* **36**, 13043–13053 (1997).
27. Woodall, D. W., Henderson, L. W., Raab, S. A., Honma, K. & Clemmer, D. E. Understanding the Thermal Denaturation of Myoglobin with IMS-MS: Evidence for Multiple Stable Structures and Trapped Pre-equilibrium States. *J Am Soc Mass Spectrom* **32**, 64–72 (2021).
28. Breuker, K. & McLafferty, F. W. Stepwise evolution of protein native structure with electrospray into the gas phase, 10−12 to 102 s. *Proceedings of the National Academy of Sciences* **105**, 18145–18152 (2008).
29. Ujma, J., Giles, K., Morris, M. & Barran, P. E. New High Resolution Ion Mobility Mass Spectrometer Capable of Measurements of Collision Cross Sections from 150 to 520 K. *Anal. Chem.* **88**, 9469–9478 (2016).
30. Berezovskaya, Y., Porrini, M. & Barran, P. E. The effect of salt on the conformations of three model proteins is revealed by variable temperature ion mobility mass spectrometry. *International Journal of Mass Spectrometry* **345–347**, 8–18 (2013).
31. Lazar, K. L., Patapoff, T. W. & Sharma, V. K. Cold denaturation of monoclonal antibodies. *mAbs* **2**, 42–52 (2010).
32. Norgate, E. L. *et al.* Cold Denaturation of Proteins in the Absence of Solvent: Implications for Protein Storage**. *Angewandte Chemie International Edition* **61**, e202115047 (2022).

33. Holehouse, A. S., Das, R. K., Ahad, J. N., Richardson, M. O. G. & Pappu, R. V. CIDER: Resources to Analyze Sequence-Ensemble Relationships of Intrinsically Disordered Proteins. *Biophysical Journal* (2017) doi:10.1016/j.bpj.2016.11.3200.

34. Fernandez de la Mora, J. Electrospray ionization of large multiply charged species proceeds via Dole's charged residue mechanism. *Analytica Chimica Acta* **406**, 93–104 (2000).

35. Jones, D. T. & Cozzetto, D. DISOPRED3: precise disordered region predictions with annotated protein-binding activity. *Bioinformatics* **31**, 857–863 (2015).

36. Beveridge, R., Chappuis, Q., Macphee, C. & Barran, P. Mass spectrometry methods for intrinsically disordered proteins. *Analyst* **138**, 32–42 (2012).

37. Konermann, L. A Minimalist Model for Exploring Conformational Effects on the Electrospray Charge State Distribution of Proteins. *J. Phys. Chem. B* **111**, 6534–6543 (2007).

38. Badman, E. R., Hoaglund-Hyzer, C. S. & Clemmer, D. E. Dissociation of different conformations of ubiquitin ions. *J Am Soc Mass Spectrom* **13**, 719–723 (2002).

39. Koeniger, S. L. & Clemmer, D. E. Resolution and Structural Transitions of Elongated States of Ubiquitin. *Journal of the American Society for Mass Spectrometry* **18**, 322–331 (2007).

40. Jung, J. E. *et al.* Differentiation of Compact and Extended Conformations of Di-Ubiquitin Conjugates with Lysine-Specific Isopeptide Linkages by Ion Mobility-Mass Spectrometry. *J. Am. Soc. Mass Spectrom.* **22**, 1463–1471 (2011).

41. Shi, H. & Clemmer, D. E. Evidence for Two New Solution States of Ubiquitin by IMS–MS Analysis. *J. Phys. Chem. B* **118**, 3498–3506 (2014).

42. El-Baba, T. J. *et al.* Melting Proteins: Evidence for Multiple Stable Structures upon Thermal Denaturation of Native Ubiquitin from Ion Mobility Spectrometry-Mass Spectrometry Measurements. *J. Am. Chem. Soc.* **139**, 6306–6309 (2017).

43. Faizullin, D. A., Konnova, T. A., Haertle, T. & Zuev, Yu. F. Self-assembly and secondary structure of beta-casein. *Russ J Bioorg Chem* **39**, 366–372 (2013).

44. Wood, S. J. *et al.* α-Synuclein Fibrillogenesis Is Nucleation-dependent: IMPLICATIONS FOR THE PATHOGENESIS OF PARKINSON'S DISEASE *. *Journal of Biological Chemistry* **274**, 19509–19512 (1999).

45. Zhou, X. *et al.* Star-Shaped Amphiphilic Hyperbranched Polyglycerol Conjugated with Dendritic Poly(l -lysine) for the Codelivery of Docetaxel and MMP-9 siRNA in Cancer Therapy. *ACS Applied Materials and Interfaces* **8**, 12609–12619 (2016).
46. Hochstrasser, M. Origin and function of ubiquitin-like proteins. *Nature* **458**, 422–429 (2009).
47. Beta-Casein - an overview | ScienceDirect Topics. https://www.sciencedirect.com/topics/agricultural-and-biological-sciences/beta-casein.
48. Bendor, J., Logan, T. & Edwards, R. H. The Function of α-Synuclein. *Neuron* **79**, 10.1016/j.neuron.2013.09.004 (2013).
49. Beveridge, R. *et al.* Ion Mobility Mass Spectrometry Uncovers the Impact of the Patterning of Oppositely Charged Residues on the Conformational Distributions of Intrinsically Disordered Proteins. *J. Am. Chem. Soc.* **141**, 4908–4918 (2019).
50. Das, R. K. & Pappu, R. V. Conformations of intrinsically disordered proteins are influenced by linear sequence distributions of oppositely charged residues. *Proceedings of the National Academy of Sciences* **110**, 13392–13397 (2013).
51. Wang, X. *et al.* Exploring the Conformational Landscape of Poly(L-lysine) Dendrimers using Ion Mobility Mass Spectrometry. Preprint at https://doi.org/10.26434/chemrxiv-2023-jvp7r (2023).
52. Jain, M. K., Singh, P., Roy, S. & Bhat, R. Comparative Analysis of the Conformation, Aggregation, Interaction, and Fibril Morphologies of Human α-, β-, and γ-Synuclein Proteins. *Biochemistry* **57**, 3830–3848 (2018).
53. Campen, A. *et al.* TOP-IDP-scale: a new amino acid scale measuring propensity for intrinsic disorder. *Protein Pept Lett* **15**, 956–963 (2008).
54. Gabelica, V. & Marklund, E. Fundamentals of ion mobility spectrometry. *Curr Opin Chem Biol* **42**, 51–59 (2018).
55. Kemper, P. R. & Bowers, M. T. Electronic-state chromatography: application to first-row transition-metal ions. *J. Phys. Chem.* **95**, 5134–5146 (1991).
56. Gabelica, V. & Marklund, E. Fundamentals of ion mobility spectrometry. *Current Opinion in Chemical Biology* **42**, 51–59 (2018).

57. Kinnear, B. S., Hartings, M. R. & Jarrold, M. F. Helix Unfolding in Unsolvated Peptides. *J. Am. Chem. Soc.* **123**, 5660–5667 (2001).

58. St. Louis, R. H., Hill, H. H. & Eiceman, G. A. Ion Mobility Spectrometry in Analytical Chemistry. *Critical Reviews in Analytical Chemistry* **21**, 321–355 (1990).

59. Eiceman, G. A. Advances in Ion Mobility Spectrometry: 1980—1990. *Critical Reviews in Analytical Chemistry* **22**, (1991).

60. Beveridge, R. *et al.* A Mass-Spectrometry-Based Framework To Define the Extent of Disorder in Proteins. *Anal. Chem.* **86**, 10979–10991 (2014).

61. Jumper, J. *et al.* Highly accurate protein structure prediction with AlphaFold. *Nature* **596**, 583–589 (2021).

62. Poyer, S. *et al.* Conformational Dynamics in Ion Mobility Data. *Anal. Chem.* **89**, 4230–4237 (2017).

63. Kalapothakis, J. M. D. *et al.* Unusual ECD fragmentation attributed to gas-phase helix formation in a conformationally dynamic peptide. *Chem. Commun.* **50**, 198–200 (2013).

64. Kim, D.-H., Lee, J., Mok, K. H., Lee, J. H. & Han, K.-H. Salient Features of Monomeric Alpha-Synuclein Revealed by NMR Spectroscopy. *Biomolecules* **10**, 428 (2020).

65. Ulmer, T. S., Bax, A., Cole, N. B. & Nussbaum, R. L. Structure and Dynamics of Micelle-bound Human α-Synuclein*. *Journal of Biological Chemistry* **280**, 9595–9603 (2005).

66. Anderson, V. L., Ramlall, T. F., Rospigliosi, C. C., Webb, W. W. & Eliezer, D. Identification of a helical intermediate in trifluoroethanol-induced alpha-synuclein aggregation. *Proceedings of the National Academy of Sciences* **107**, 18850–18855 (2010).

67. Binolfi, A., Theillet, F.-X. & Selenko, P. Bacterial in-cell NMR of human α-synuclein: a disordered monomer by nature? *Biochem Soc Trans* **40**, 950–954 (2012).

68. Sung, Y.-H. & Eliezer, D. Structure and dynamics of the extended-helix state of alpha-synuclein: Intrinsic lability of the linker region. *Protein Science* **27**, 1314–1324 (2018).

69. Bartels, T., Choi, J. G. & Selkoe, D. J. α-Synuclein occurs physiologically as a helically folded tetramer that resists aggregation. *Nature* **477**, 107–110 (2011).

70. Yu, H., Han, W., Ma, W. & Schulten, K. Transient β-hairpin formation in α-synuclein monomer revealed by coarse-grained molecular dynamics simulation. *J Chem Phys* **143**, 243142 (2015).
71. Lantz, C. *et al.* Characterization of Molecular Tweezer Binding on α-Synuclein with Native Top-Down Mass Spectrometry and Ion Mobility-Mass Spectrometry Reveals a Mechanism for Aggregation Inhibition. *J. Am. Soc. Mass Spectrom.* **34**, 2739–2747 (2023).

Acknowledgements

We acknowledge the support of EPSRC through the strategic equipment award EP/T019328/1 and for the Prosperity Partnership award EP/S005226/1, the European Research Council for funding the MS SPIDOC H2020-FETOPEN-1-2016-2017-801406 and Waters Corporation for their continued support of mass spectrometry research within the Michael Barber Centre for Collaborative Mass Spectrometry. F.B. acknowledges the Department of Chemistry and AstraZeneca for funding a strategic CASE studentship. The authors also thank the staff in the MS and Separation Science facility, in the faculty of Science and Engineering for their assistance. EN is grateful for funding through a University of Manchester Alumni Impact award and from Bristol Myers Squib.

Author contributions

XW Design of experiment; data collection, processing and analysis; drafting, editing of article. JD Data analysis and interpretation. EN, FB and JK: data collection and editing of article. RE and TB Sample Preparation. PEB supervision of project, data analysis and interpretation; design of experiment; editing of article. All authors contributed to the final submitted draft.

Competing interests

RE and TB are both employees of AstraZeneca and own or have the option to own stocks in this company.

Materials & Correspondence

Data availability

Raw data files are hosted on Figshare.